

Curvature fluctuations and the Lyapunov exponent at melting

Vishal Mehra and Ramakrishna Ramaswamy

School of Physical Sciences, Jawaharlal Nehru University, New Delhi 110067, India

(Received 28 March 1997)

We calculate the maximal Lyapunov exponent in constant-energy molecular-dynamics simulations at the melting transition for finite clusters of 6–13 particles (model rare-gas and metallic systems) as well as for bulk rare-gas solids. For clusters, the Lyapunov exponent generally varies linearly with the total energy, but the *slope* changes sharply at the melting transition. In the bulk system, melting corresponds to a jump in the Lyapunov exponent, and this corresponds to a singularity in the variance of the curvature of the potential-energy surface. In these systems there are two mechanisms of chaos—local instability and parametric instability. We calculate the contribution of the parametric instability toward the chaoticity of these systems using a recently proposed formalism. The contribution of parametric instability is a continuous function of energy in small clusters but not in the bulk where the melting corresponds to a decrease in this quantity. This implies that the melting in small clusters does not lead to enhanced local instability. [S1063-651X(97)11508-2]

PACS number(s): 05.45.+b, 36.40.-c, 64.60.My, 05.20.-y

I. INTRODUCTION

In recent years the dynamics of finite condensed-matter systems, especially atomic and molecular clusters, has been extensively studied from a nonlinear dynamics perspective [1]. Various quantities of interest like Lyapunov exponents, Lyapunov spectra, distributions of finite-time Lyapunov exponents, and the Kolmogorov entropy have been computed to see the evolution of chaoticity and ergodicity. Very general considerations lead to the expectation that the Lyapunov exponents and the Kolmogorov entropy should increase with energy. However, there are indications that different systems can display a variety of behaviors, and details of how such indices change and the different kinds of possible (qualitative as well as quantitative) behaviors—the various universality classes, so to speak—have not yet been completely characterized.

In the present work we calculate the largest Lyapunov exponent Λ for small rare-gas and metal clusters [modeled, respectively, by the Lennard-Jones (LJ) and the many-body Gupta [2] potentials] as well as for bulk rare-gas solid, namely 256 LJ atoms in a box with periodic boundary conditions. In the range studied, Λ is generally linearly related to energy (except at very low energies), but shows a sharp change in slope at an energy which can be related to the melting transition.

We also compute an estimate for Λ through a semiempirical methodology provided by a recently proposed geometrical theory of Hamiltonian chaos [3]. Under certain approximations this allows for the estimation of the relative contribution of stable modes of a Hamiltonian system toward chaotic behavior. The approximations inherent in the theory [3] are fulfilled in bulk systems (where N is large), but do not appear entirely satisfactory in small clusters. This geometrical theory has as its input the curvature of the configuration space manifold and its fluctuation. These quantities and their variation with temperature are themselves interesting because they yield a statistical quantification of the potential-energy surface. Recent approaches to the computation of Lyapunov exponents from (local) instantaneous mode analy-

sis [4,5] use this information implicitly.

The simplest understanding of chaotic dynamics in such (Hamiltonian) systems is the standard KAM picture [6]. When the number of freedoms becomes large (for 13 atoms, the phase space is 78 dimensional) the picture of a phase space foliated by tori, with surrounding stochastic regions [6] is not particularly relevant. However, the motion for specific initial conditions remains nearly periodic, while for others there can be a positive Lyapunov exponent. In particular the KAM theorem underestimates the chaotic thresholds by several orders of magnitudes [7] in high-dimensional systems as the critical perturbation scales as $\sim \exp(-\alpha N_f)$ which rapidly goes to zero with increasing N_f (degrees of freedom), contrary to the experience in numerical simulations beginning with Fermi, Pasta, and Ulam's famous result [8]. Also, attainment of chaoticity does not exhaust the interest in dynamics—in particular the evolution of the dynamics near a thermodynamic phase transition is nontrivial. At energies corresponding to the phase-transition phenomenon, the accessible phase space increases greatly, and correspondingly Λ shows a signature of the transition. An alternate means of analysis is through decorrelation of the eigenvectors of the instantaneous Jacobian along a trajectory [4]. The time scale for this process is greatly reduced by the presence of the regions of negative curvature (unstable modes), which also increase at the melting phase-transition point.

Such ideas have been at the root of a variety of studies of the Lyapunov exponent or related quantities. Posch and Hoover [9] calculated Lyapunov spectra of solid and liquid LJ systems in two and three dimensions, and attempted to fit a power law to this data, obtaining different exponents in the solid and liquid phases, although no definite significance could be ascribed to these. Berry and co-workers [10] examined a variety of quantities including finite-time or local approximations to Kolmogorov entropy and Lyapunov spectrum in LJ and Morse clusters containing between three and 13 particles [10]. These studies have been able to make contact between the features of the potential-energy surface and the variation of different dynamical indicators. Recently Sastri [4] computed the maximal Lyapunov exponent as well as

the entire Lyapunov spectra for a 32-atom Lennard-Jones fluid in the temperature range 50–800 K. A power-law fit of Λ with temperature does not yield a single exponent but a crossover (around $T=1$) between the exponent = 1 at low temperature to $\frac{1}{2}$ at high temperatures [11]. In a finite lattice system, Butera and Caravati [12] simulated the coupled rotor system in two dimensions which has a Kosterlitz-Thouless (KT) transition at constant energy and observed that the scaling of Λ with the temperature changes at precisely the KT temperature. Recent simulations on the XY model in two and three dimensions by Caiani *et al.* [13] showed the differences between the KT transition and a true symmetry-breaking transition in three dimensions. The crossover in scaling of Λ with temperature or energy per particle, also observed in other lattice models where it had purely dynamical significance [14], was suggested to coincide with the crossover from slow to fast diffusion in the phase space [7], and was labeled as the strong stochasticity threshold (SST). The generality of the SST in nonlinear Hamiltonian systems is not obvious, although it appears to persist even for large degrees of freedom in the models studied. It was also found that SST occurs in lattice models with Lennard-Jones interactions in two and three dimensions [15], the signature being a rapid relaxation of the specific heat and independence of Λ on the initial conditions. Similar transitions have also been observed in small rare-gas and metal clusters [16]. A somewhat different interpretation of these results has also been proposed [17].

In small rare-gas atomic clusters, Λ has been calculated at the melting transition [18], which is a finite-size analog of the bulk melting transition [19]. Whereas Λ changes discontinuously with energy for LJ₁₃ and LJ₅₅, for LJ₇ the slope changes discontinuously. At the energy of this change, indicators of melting like Lindemann index or density of states show characteristic signature, so it was proposed that Λ is a good indicator of melting transition [18,20]. Subsequent work [21] has revealed that the behavior of Λ as a function of the energy is more complicated, and can be different depending on the nature of the low-energy configuration that the system starts from. More recently Dellago and Posch [22] calculated Λ , the Lyapunov spectra, and related quantities like the fraction of unstable modes for the melting transition of certain modified LJ systems in two dimensions. They found that Λ has a broad peak near the melting density and a steplike increase at the melting temperature, and further suggested that there is a change in the shape of the Lyapunov spectra at the transition density. Critical phenomena which occur at higher temperatures in larger fragmenting clusters have also been studied [23], although the claimed form for the (finite-time) Lyapunov exponent, namely, $\Lambda \sim (T - T_c)^{-\mu}$, with universal behavior for μ , is questionable [13,24].

Our work in the present paper is focused on the study of clusters and bulk at the melting transition, with particular emphasis on the Lyapunov exponent and the curvature fluctuations. In Sec. II, we examine the behavior of Λ , and in Sec. III, the nature of the curvature fluctuations are analyzed in order to make contact between theory and simulations. The methodology and theoretical background for the extraction of Λ from curvature data is elaborated upon in Sec. III where our results for bulk as well as cluster systems are also

presented. This is followed by a summary and discussion in Sec. IV.

II. MELTING AND LYAPUNOV EXPONENT IN CLUSTERS AND BULK

As is by now well known [25], atomic clusters with as few as six or seven particles undergo a finite-size analog of the bulk melting phase transition, which is marked by a jump in the Lindemann index and the onset of rapid isomerization. The liquidlike phase of the small clusters is, however, unlike the bulk liquid in one important respect: due to the phase-space constraints, the atomic displacements (“hopping processes”) are highly correlated, giving rise to $1/f$ spectra of single-particle potential-energy fluctuations [26]. It has been observed that in metal clusters particles can occupy two types of sites—of low and high energy, respectively, and the onset of the liquid phase corresponds to the onset of an isomerization occurring through four-particle interchange between high- and low-energy sites [27]. Similar features are also expected for rare-gas clusters. This peculiar dynamics has interesting consequences which we examine in this section.

We consider clusters of up to 13 atoms interacting via the LJ potential

$$V = 4\epsilon \sum_{i < j} \left[\left(\frac{\sigma}{r_{ij}} \right)^{12} - \left(\frac{\sigma}{r_{ij}} \right)^6 \right], \quad (1)$$

which is appropriate for rare-gas atoms; we work in reduced units when $\sigma = \epsilon = 1$. In order to model metallic clusters, the many-body Gupta (Gu) potential [2]

$$V = (1/2)U \sum_j \left\{ A \sum_i \exp[-p(r_{ij} - r_0)] - \left[\sum_i \exp[-2q(r_{ij} - r_0)] \right]^{1/2} \right\} \quad (2)$$

is commonly used. Here r_{ij} is the distance between the atoms i and j , and r_0 is the interatomic distance in the bulk (fcc) crystal. The specific metallic cluster system we model corresponds notionally to Ni, for which we use parameters given in Ref. [25]: $p=9/r_0$, $q=3/r_0$, $A=0.101\,035$, and $U/E_{\text{bulk}}=0.855\,05$ (E_{bulk} is the bulk cohesive energy of the metal by which all energies are scaled). Quantities like Λ and Kolmogorov-Sinai entropy have been calculated for small rare-gas clusters and the relation of the potential-energy surface to local dynamical behavior has been analyzed [10,28]. In particular it is known that smooth saddles cause a drop in local chaoticity indicators [10].

Time is measured in units of $(m\sigma^2/\epsilon)^{1/2}$ for LJ clusters and $(mr_0^2/E_{\text{bulk}})^{1/2}$ for Gupta clusters. Constant energy simulations are done using the Verlet algorithm with step size $\Delta t=0.01$ in these units, and the total energy is conserved to 0.01%. The total integration time varies between $10^5 \Delta t$ to $5 \times 10^5 \Delta t$ depending on the potential and the system size. Simulations start at the global minimum of the structure, and then gradually move up in energy; at the highest temperatures studied evaporation does not set in within the time period of the computation. Temperature is defined in the

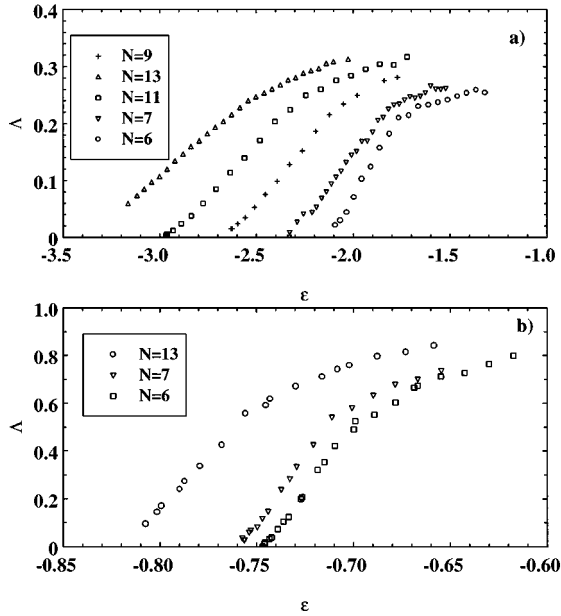


FIG. 1. (a) Λ as the function of reduced energy per particle for LJ clusters with $N=6, 7, 9, 11,$ and 13 . Note that the list includes both magic and nonmagic clusters. (b) Λ for Gu clusters with $N=6, 7,$ and 13 . The reduced energy scale is set by E_{bulk} [Eq. (2)].

usual manner, as proportional to the average kinetic energy per particle, $T=2\langle E_k\rangle/[k_B(3N-6)]$, k_B being the Boltzmann constant.

At very low energies the dynamics is nonergodic; in particular, for 13-particle clusters the nonergodicity can be persistent up to rather high energies. The breathing mode in LJ_{13} was recently studied in Ref. [29]. This mode is stable (i.e., nondecaying) up to an energy $E=0.150$ per particle above the global minimum; the corresponding mode for LJ_7 survives only up to energy 0.042 above the minimum. Stability here is tested by starting trajectories with an isotropic stretching of the global minimum structure. In this nonergodic region the system initialized with a small random distortion of the icosahedral structure has a very small positive Lyapunov exponent, while, for larger distortions at the same energy, Λ can be much larger. As energy increases, the overall cluster distortions increase, and this mode becomes markedly unstable. For large initial distortions from icosahedral geometry of LJ_{13} , a chaotic transition occurs at a lower energy and is manifested as the divergence of the microcanonical specific heat [16]. This energy depends on the equilibration time, but tends to a nonzero value for large equilibration times. Such transitions are not size specific, and have been seen for nonmagic clusters as well.

Figure 1 shows the variation of $\Lambda(\epsilon)$ with the reduced energy per particle, ϵ , for LJ and Gu clusters of various sizes. At higher energies $\Lambda(\epsilon)$ is linear but at a certain energy a sharp change in the slope is evident in all cases. Precisely at this energy the conventional criterion of melting applies, namely, the Lindemann index crosses the value 0.1 (Lindemann indices for Gu clusters were studied in Ref. [25]). In LJ_{13} , which has a large solid-liquid coexistence region between $-2.6 < \epsilon < -2.2$, Λ changes slope at $\epsilon \approx -2.6$. In LJ_6 , where the Lindemann index increases continuously, the discontinuity in Λ appears just after the Lin-

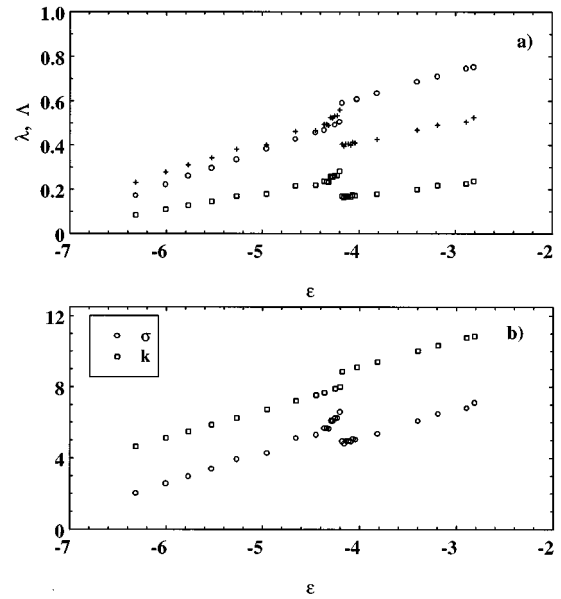


FIG. 2. (a) Lyapunov exponents for the bulk LJ system of 256 particles in a cubical box with periodic boundary conditions. Circles refers to Λ , and squares to the estimate λ generated using Eq. (8), with τ defined in Eq. (10). Pluses (+) denote values of λ calculated using $\tau_2 = k^{1/2}/\sigma$. (b) Mean curvature (k), and fluctuation σ for the bulk LJ system as a function of energy. k and σ are measured in units of frequency squared.

demann index has reached its critical value 0.1. The slope in the liquid phase is always smaller, indicating that the diffusive modes have different chaotic properties, giving rise to different energy dependence of Λ . The change in the slope of $\Lambda(\epsilon)$ can also be taken to be a characteristic signature of melting in small clusters. The slope of the $\Lambda(\epsilon)$ curves are generally smaller for the larger cluster; furthermore, the sharpness of the discontinuity (in slope) is reduced as the cluster size increases.

For the Gupta clusters, however, these trends with N are not strongly marked, which is a consequence of the many-body character of the Gu potential: even if a pair of particles is not interacting directly (being outside the potential cutoff), the corresponding elements of the Hessian matrix need not vanish because of the many-body term. We find that the slope changes distinctly at an energy corresponding to the top of the jump in the Lindemann curve.

The third system we study is bulk, and Fig. 2(a) shows $\Lambda(\epsilon)$ for the system of 256 LJ particles in a cubic box with periodic boundary conditions at the reduced density $\rho=0.93$ and reduced melting temperature 1.15. Initial conditions for these simulations were as follows: the atoms were initially at fcc lattice positions, with initial velocities taken randomly from an appropriate Gaussian distribution. For $\epsilon > -4.25$ the crystal is unstable and soon melts. It is possible for melting to occur for slightly lower energies if integration is carried for longer times, but the time required to melt is not a monotonically decreasing function of energy. Here $\Lambda(\epsilon)$ shows a jump which obviously can be ascribed to the increase in the disorder at melting. The data shown are the Lyapunov exponent of the solid- or liquid-phase trajectory only, which are obtained by discarding the premelting portion of a trajectory that melts. Similar results for bulk

melting have also been reported in Refs. [22] and [30].

While both the bulk and the cluster are disordered by melting (change in entropy at melting, $\Delta S/N=1.0$ for the LJ₅₅ and 1.7 for the LJ crystal [19], and the specific heat of even a six-particle cluster shows a peak), Λ in the cluster liquid phase is significantly smaller than the value obtained by extrapolating from the solid phase, in contrast with Λ obtained in bulk liquid. This suggests that in the cluster liquid phase there are stabilizing influences on the dynamics which are absent in the bulk liquid. We conjecture that the correlated hopping processes in clusters [26,27] provide the necessary mechanism. This is consistent with the observation made above that the $\Lambda(\epsilon)$ curve becomes smoother with the cluster size.

The observed Lyapunov phenomenon for the clusters is not just an effect of the smeared-out bulk transition, i.e., a manifestation of finite dynamical coexistence region in the clusters which vanishes in the bulk limit. The properties of the coexistence region (in particular its width) depend sensitively on the cluster geometry, e.g., the fact that the cluster is magic or not. But the trends in the Lyapunov exponent depend on the size in a simple manner and are independent of the magic-nonmagic relation.

The spectra of $3N-7$ positive Lyapunov exponents for the clusters vary smoothly with energy. For LJ clusters they are linear in the entire range with a slope that increases with energy, while in Gu clusters they acquire increasing curvature. This is in contrast to the results of Dellago and Posch [22] for bulk melting in two dimensions, where the curvature of the spectra changes sign smoothly at certain densities (at constant temperature). It remains a task to extract more useful information from the shape of the Lyapunov spectra. However, the smoothness of the spectra at cluster melting implies that the relation (if any) between thermodynamic and dynamic entropies is nontrivial.

III. CURVATURE FLUCTUATIONS

In this section we apply the geometric theory of Hamiltonian chaos developed by Pettini and co-workers [3] in order to interpret and rationalize the results of our numerical simulations in terms of an underlying (microscopic) mechanism. This theory, the salient features of which are summarized below, is attractive because it attempts to unite features of the potential-energy surface with the dynamical properties of the system as encoded in the Lyapunov exponents. One additional motivation in applying this theory to finite cluster systems is to determine the limits of applicability of the general framework, which has mainly been applied to lattice models where the calculated Lyapunov exponents are found to be in good agreement with empirical exponents [3,13].

A. Geometric theory of chaos in high-dimensional systems

It is well known that the classical dynamics on manifolds of constant negative curvature is chaotic [31]. The dynamics on a manifold with fluctuating positive curvature can also be chaotic [32]: this fluctuation, via the mechanism of parametric instability, is responsible for creating chaos in systems such as the Fermi-Pasta-Ulam β and ϕ^4 chains [7], and for a driven one-dimensional oscillator studied in Ref. [33]. These studies have provided much of the motivation for the devel-

opment of the geometric theory of chaos [3]. Barnett *et al.* [34] applied similar ideas to a calculation of the Lyapunov exponent of a dilute gas.

The geometric theory makes a diagonal approximation in the sense that it uses information only about the trace of the instantaneous Hessian matrix, i.e., ΔV . When the equations of motion are put in a differential-geometric form, this term appears as the Ricci curvature (curvature locally averaged over the directions) of the enlarged configuration manifold in the Eisenhart metric [3],

$$ds^2 = -2V(q)dt^2 + a_{ij}dq^i dq^j + dt dq^{N_f+1}. \quad (3)$$

Here $V(q)$ is the potential energy and the kinetic energy is $T = a_{ij}\dot{q}^i \dot{q}^j$. The relevance of potential curvature has been noted before [35]. The Ricci curvature does not have this simple form in other metrics, but the essence of the assumption is that all the directions in the phase space are equally curved after a coarse graining along a trajectory. The dynamical trajectories are the geodesics of this manifold. In above models this appears to be the dominant mechanism for chaos as there are no unstable modes (corresponding to the negative eigenvalues of the instantaneous Hessian matrix or regions of negative curvature), which are the *local* mechanism of chaos.

If it is assumed that the curvature fluctuations have Gaussian spectra up to a high-frequency cutoff, i.e., the dynamics generates a Gaussian random process for curvatures, then one can dispense with the necessity of following a trajectory and an estimate of the largest Lyapunov exponent, λ can be obtained via Monte Carlo sampling. This is the essence of the Gaussian approximation [3], within which excellent agreement is obtained between Λ and λ . The presence of additional unstable modes renormalizes the calculated exponent, although this is nontrivial to calculate. Therefore the unrenormalized exponent gives an estimate of the chaoticity caused by stable modes only (the unstable modes also contribute to parametric instability by their presence in ΔV , but it is not their major effect on chaoticity). The theoretical basis of the diagonal approximation assumption is that the local fluctuation of the Ricci curvature detects deviation from isotropy (at a point) because isotropic manifolds are necessarily of constant curvature by Schur's theorem [3].

The crossover between the regimes of weak and strong chaos in high-dimensional systems can be detected by examining the behavior of the mean curvature, k , as a function of the energy density. In the integrable limit k is independent of energy [3]. Corresponding to a Hamiltonian H of N particles with an interaction V ,

$$H = \sum_i \frac{p_i^2}{2} + V(q), \quad (4)$$

there are $3N$ equations of motion:

$$\frac{d^2 q_i}{dt^2} = - \frac{\partial V}{\partial q_i}. \quad (5)$$

The associated Jacobi equation for the second deviations is then

$$\frac{d^2 J_i}{dt^2} + \sum_j \frac{\partial^2 V}{\partial q_i \partial q_j} J_j = 0, \quad (6)$$

where J_i are the components of the vector of second deviations. After some approximations [3], this can be converted to an equation for $u = |J|$,

$$\frac{d^2 u}{dt^2} + \sum_{ij} \frac{\partial^2 V}{\partial q_i \partial q_j} \frac{J_i J_j}{|J|^2} u \equiv \frac{d^2 u}{dt^2} + Q(t)u = 0, \quad (7)$$

which is, in effect, an equation for a linear oscillator with time-dependent frequency \sqrt{Q} . The solutions of this equation are unbounded for typical $Q(t)$ and the Lyapunov exponent is just given by the rate of exponential growth of the envelope of u [36]. Pettini and co-workers [3] showed that $Q(t)$ is just the sectional curvature (which is the generalization of Gaussian curvature to many dimensions) relative to the plane containing J and dq/dt in the Eisenhart metric. The diagonal approximation consists in replacing Q by the simpler quantity

$$\frac{\Delta V}{N_f} = \frac{1}{N_f} \sum_i \frac{\partial^2 V}{\partial q_i^2}, \quad (8)$$

with N_f the number of degrees of freedom, which is [3] the Ricci curvature per degree of freedom, i.e., the sectional curvature has been averaged over relative orientations of J and the velocity vector. Under the further assumption that the curvature is Gaussian distributed with a mean $k = \langle \Delta V \rangle / N_f$ and variance $\sigma^2 = [\langle (\Delta V)^2 \rangle - \langle \Delta V \rangle^2] / N_f$ and are δ correlated, Pettini and co-workers [3] derived an expression for an estimate of the Lyapunov exponent

$$\lambda = \frac{1}{2} \left(l - \frac{4k}{3l} \right), \quad (9)$$

$$l = \left[\sigma^2 \tau + \left(\frac{64k^3}{27} + (\sigma^2 \tau)^2 \right)^{1/2} \right]^{1/3}, \quad (10)$$

where τ is a characteristic time implied by the smoothness of the underlying manifold, i.e., the time interval below which dynamics of curvatures cannot be regarded as a random process.

B. Application of the geometric theory

The main result of the geometric theory is an estimate of the Lyapunov exponent, λ given in Eq. (9), for which it is necessary to obtain the mean curvature k and the variance σ^2 . These quantities can be calculated along a typical trajectory using Eq. (8), and the assumption of δ -correlated curvature fluctuations can be directly verified.

The determination of the time scale τ [see Eq. (10)] is more tricky. One estimate which has been used [3,13,37] is

$$\tau = \frac{\pi \sqrt{k}}{2 \sqrt{k(k+\sigma)} + \pi \sigma}. \quad (11)$$

This expression for τ here is actually that for τ_* in Ref. [3] [see the discussion following Eq. (45) there]. However, in

the presence of negative curvatures it may be more accurate to use a different time scale [3],

$$\tau_2 = \frac{k^{1/2}}{\sigma}. \quad (12)$$

We find (see Sec. III C) that τ_2 is more accurate than τ insofar as it provides a better numerical match with the autocorrelation decay time scale for the systems studied here.

One additional minor point is that the effective number of freedoms is $N_f = 3N - 6$ rather than $3N$, since the six conserved quantities (linear and angular momenta) give rise to zero-frequency modes and thus do not contribute to the chaoticity. This does not change qualitative conclusions (indeed it must not), and improves results in most cases.

The application of the geometric theory to the systems considered in Sec. II is of interest for two reasons. First, this formalism has so far been mostly applied to lattice models, where parametric instability is the main source of chaos. It would be useful to determine the extent to which the formalism works for off-lattice models with significant local instability. Second, the partition of the chaoticity of the system into local and nonlocal components may help in clarifying the behavior of Lyapunov exponent at melting. In particular, it would be interesting to know whether the overall instability of the system can be separated into these two components, and, if so, whether they behave differently at phase transitions.

The melting transition in finite systems appears to have a distinct signature—the Lyapunov exponent shows a knee, where the slope changes discontinuously [20]. For bulk, the fraction of the unstable modes has a discontinuous jump at melting. Therefore a rapid increase in local instability and consequently, a jump in the Lyapunov exponent can be expected. Such a change may not be apparent in the contribution of the parametric instability, and therefore in the situation of cluster melting where Lyapunov exponent does not increase, it is an open question whether the local instability increases or not.

C. Results

As should be clear from the preceding discussion, application of the geometric theory in order to make comparison with the results of our numerical simulations involves a number of sensitive estimates and several approximations. Following the general procedure outlined in Sec. III B above, we calculated the estimate λ [cf. Eq. (9)] for bulk (LJ) and various LJ and Gu clusters in an energy range which encompasses melting, from long trajectories of duration up to $2 \times 10^6 \Delta t$. The data for k , σ and λ are shown in Figs. 2–6. The detailed comparisons of theory and simulations are presented separately for bulk and cluster systems below.

1. Bulk LJ system

Casetti and Macchi [37] have calculated the curvature for bulk LJ in an exponentially large energy range in order to detect the crossover between weakly and strongly chaotic regimes. Earlier calculations by LaViolette and Stillinger [38] of the mean curvature (which is proportional to the squared Einstein frequency) show that k increases linearly in

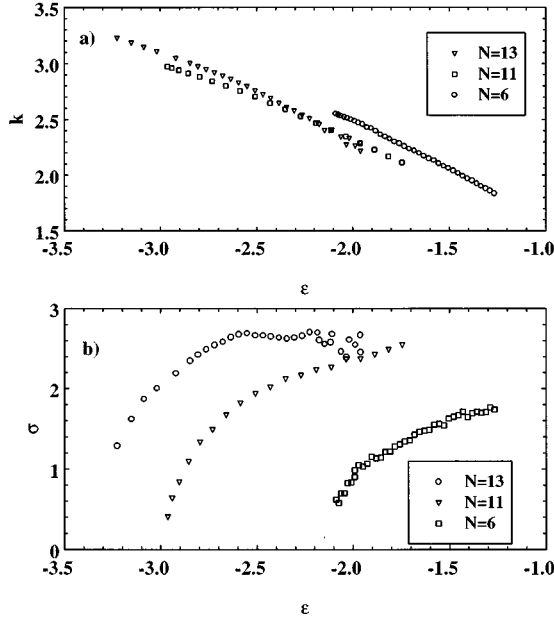


FIG. 3. (a) Mean curvature k and (b) fluctuation σ for LJ_N clusters with $N=6, 11,$ and 13 as functions of energy. Units are as in Fig. 2.

the bulk LJ system with a jump of about 20% at melting. This increase is a manifestation of the positive high-frequency tail in the instantaneous normal spectrum in the liquid phase. However, the slope in the liquid phase is smaller than the solid phase by about 6%.

We find that the variance σ^2 has a *discontinuity* at an energy $\epsilon_m = -4.17$. At energies well away from ϵ_m , σ increases linearly with energy but in a very narrow range preceding ϵ_m , roughly corresponding to the solid-liquid coexistence region, σ increases sharply. As the system melts σ falls by about 30%. (The discontinuity in σ has been confirmed by repeating the calculations with longer trajectories and finer energy mesh. Data in the coexistence region were computed from long trajectories of total time $2 \times 10^5 \Delta t$.

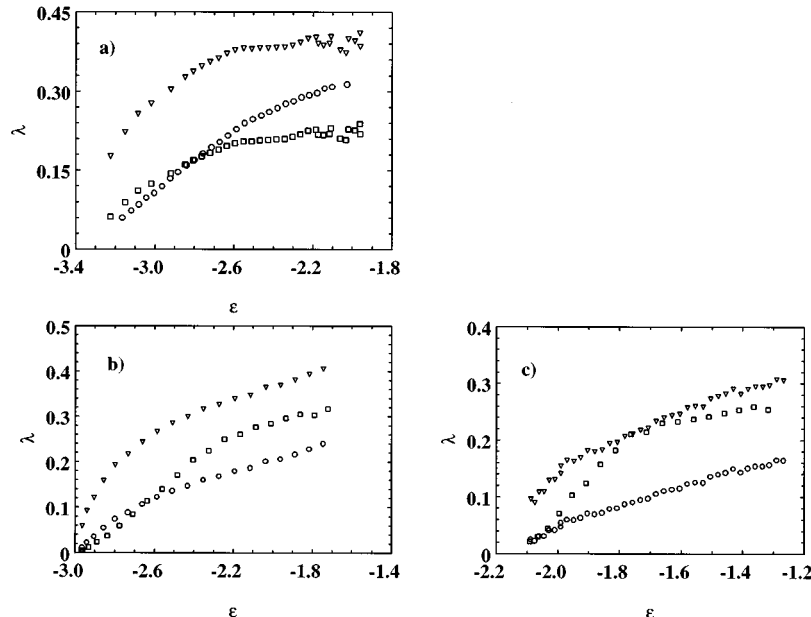


FIG. 4. The estimate λ for LJ_N clusters with $N=6, 11,$ and 13 as the function of energy. Shown with circles are λ calculated with τ defined in Eq. (10); + are values of λ calculated using $\tau_2 = k^{1/2}/\sigma$. Also, for comparison, we show the corresponding values of Λ from Fig. 1 (squares).

Care was taken to ensure that computed averages are over either the solid or liquid phase exclusively.) This behavior may be contrasted with the cusp singularity found recently in the XY model in three dimensions by Caiani *et al.* [13], which was interpreted as suggestive of a topological transition in the potential-energy surface.

The assumption of δ -correlated curvature fluctuation can be substantiated by examining the power spectra of curvature fluctuations. Figure 7 shows that these are satisfied in the bulk. However the observed correlation time does not agree with τ given in Eq. (11) (see Table I). We therefore use τ_2 to calculate the relative contribution of unstable modes, namely,

$$\delta\lambda_u \equiv (\Lambda - \lambda)/\Lambda. \quad (13)$$

Indeed $\lambda(\tau_2)$ is much better fit to Λ than $\lambda(\tau)$ (Fig. 2). $\delta\lambda_u$ can become slightly negative in the solid phase (implying some correction due to correlations), while in the liquid phase, it can be as large as 0.35. Assignment of the difference $\Lambda - \lambda$ to the effect of unstable modes is justified by the following two observations. First, λ does not increase at melting (it actually falls), whereas Λ has significant jump which can be accounted for by an increase in the fraction of unstable modes. In addition, the agreement of λ and Λ is better at lower temperatures, namely, when the occurrence of negative curvatures is infrequent.

2. Clusters

Owing to the finiteness of cluster systems, correlations do not decay sufficiently rapidly [27]. As a consequence, curvature fluctuations are far from being uncorrelated, and the framework of the geometric theory breaks down for such systems and deviations from Eq. (9) can be expected. The observed correlation times do not agree with analytical estimates for τ and τ_2 (Table I).

The mean curvature for specific LJ clusters has been computed previously [39,40], and, in contrast to bulk, decreases uniformly with energy for all clusters (except LJ_{13}); likewise

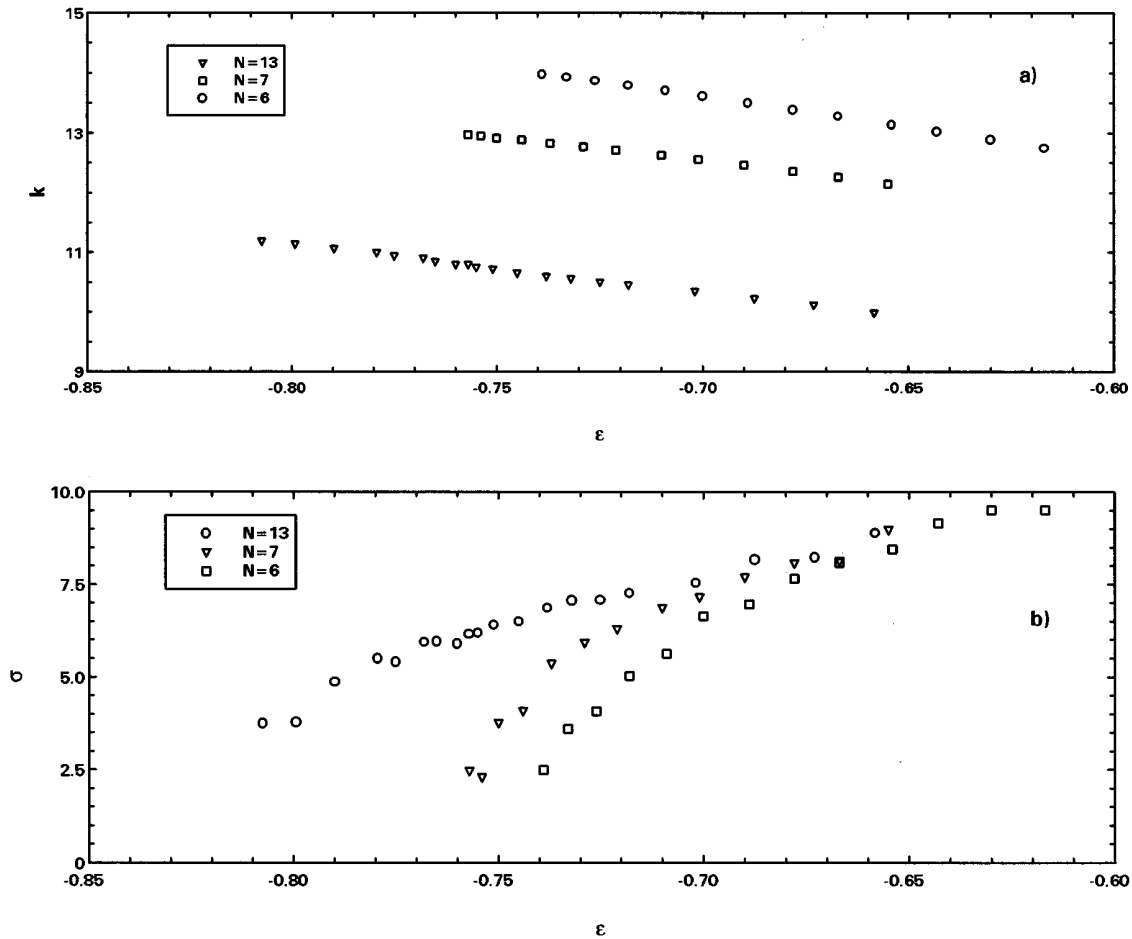


FIG. 5. (a) Mean curvature (k) and (b) fluctuation (σ) Gu_N clusters with $N=6, 7,$ and 13 as a function of energy. k and σ are scaled by E_{bulk}/mr_0^2 .

for Gupta clusters. No trend is apparent either for k or its variation with energy, although there are some size effects in the case of Gupta clusters. The behavior of the variance σ^2 is more complex. Although this quantity usually increases

smoothly with energy, in the coexistence regime near melting there are large fluctuations which persist for very long averaging times. The liquid phase in LJ_{13} also shows a non-monotonic dependence of variance on energy.

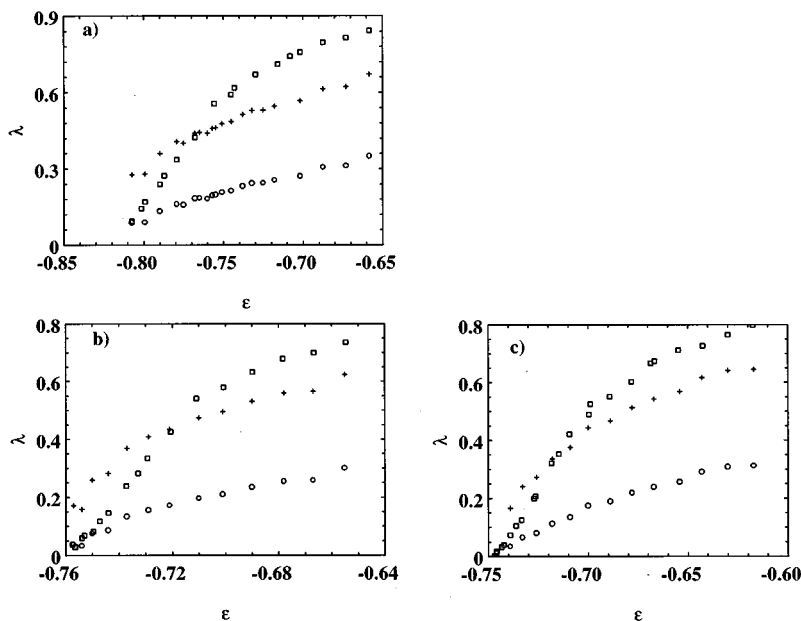


FIG. 6. The estimate λ for Gu_N clusters with $N=6, 7,$ and 13 as a function of energy (same conventions as Fig. 4).

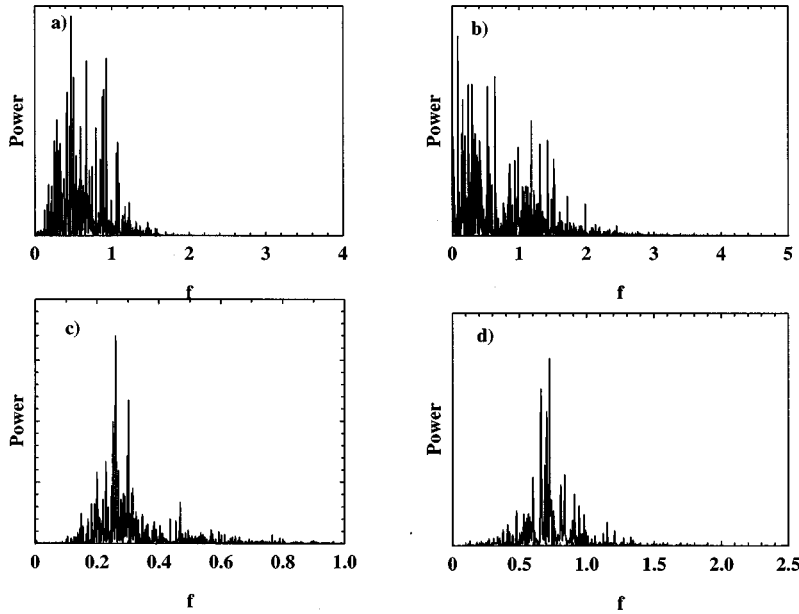


FIG. 7. Power spectra of curvature distribution calculated along a trajectory for (a) bulk LJ (solid), (b) bulk LJ (liquid), (c) LJ₁₃ at an energy of -2.4 corresponding to the temperature 34 K (coexistence region), and (d) Gu₁₃ at $\epsilon = -0.67$ (liquid phase). The vertical axis is in arbitrary units.

The net result of the persistence of correlations is that the estimates λ for cluster systems do not agree with Λ . While $\lambda(\tau)$ is a rather good fit for LJ clusters, it is of doubtful validity because τ is far from the observed fluctuation time-scale τ_c (Table I). Using τ_2 in Eq. (9) gives $\lambda/\Lambda \approx 1.3-2.5$ for LJ clusters, although for the tightly bound Gupta clusters, this discrepancy is smaller, $\lambda/\Lambda \approx 0.8-1.2$.

3. Discussion

Our results indicate that unstable modes have suppressed chaoticity in certain circumstances. In particular, in the solid LJ system, where $\delta\lambda_u$ is very small, the fraction of unstable modes is substantial (~ 0.2), while a slightly higher ($\sim 0.25-0.3$) fraction of unstable modes in liquid gives a

TABLE I. Typical time scales (in reduced units) associated with power spectra for various systems studied here.

System	τ^a	τ_2^b	τ_B^c	τ_c^d	Λ
Gu ₆ solid	0.30	1.5	0.8	2.0	0.2
Liquid	0.18	0.4	0.7	1.1	0.7
Gu ₁₃ solid	0.28	0.9	0.8	1.4	0.3
Liquid	0.18	0.36	0.7	0.9	0.8
LJ ₆ solid	0.55	1.6	2.5	10.	0.05
Liquid	0.4	0.8	1.0	1.0	.25
LJ ₁₃ solid	0.5	1.4	1.7	2.5	0.1
Liquid	0.3	0.6	1.0	1.0	0.3
Bulk solid	0.2	0.5	0.6	0.6	0.3
Liquid	0.2	0.6	0.4	0.4	0.8

^aCalculated with Eq. (10).

^bCalculated with Eq. (11).

^cObtained from approximate upper cutoff of the power spectrum.

^dInverse bandwidth of the power spectrum (approximate).

greatly enhanced value of $\delta\lambda_u$ (~ 0.35). In the cluster, even after melting, $\delta\lambda_u$ does not increase very much: it has a smooth dependence on energy. A tentative conclusion that can be drawn from these cases is that unstable modes have effective chaoticity only when the particles are free to execute large-scale motion.

If the coarse-grained curvature is everywhere positive, the ratio σ/k provides a crude measure of the ruggedness or roughness of the underlying potential-energy surface. As it is this feature which causes nearby trajectories to diverge, it is interesting to study the variation of this index with energy, as this will give some indication of the nature of the region that is being dynamically probed on the potential-energy surface.

At low energies σ/k is small, as expected, typical values being $\sim 0.2-0.4$. At the highest energies reached, it is between 0.8 and 1.2 for various clusters with somewhat higher values for LJ clusters and smaller N . In the bulk system, a peak $\sigma/k \approx 0.8$ is reached at the melting point (from the solid phase), and then it remains nearly constant. The correspondence of the maximal roughness with the melting point is very suggestive. One can visualize destruction of the crystal lattice being driven by large-scale roughness of the potential.

IV. CONCLUSION

In this paper we have examined the behavior of the largest Lyapunov exponent Λ as a function of energy in finite clusters of 6–13 rare-gas and metal atoms, and in bulk rare-gas solids. These systems undergo a phase transition from a regime wherein the dynamics is purely oscillatory (involving individual particle vibrations) to a regime where the dynamics is both oscillatory as well as diffusive.

Diffusive dynamics is linked to the presence of delocalized unstable modes in the bulk [41]. In small clusters the onset of the diffusion does not appear to enhance the chaoticity: the observed value of the Lyapunov exponent is smaller compared to the value expected by a simple extrapolation of the exponent from the low-energy regime, namely, from the oscillatory dynamics or the “solid” phase. This

suppression of chaos, which we attribute to the correlated hopping dynamics, is strongest for smallest clusters but is then progressively reduced. It is possible that, for particular clusters, the enhancing and suppressing effects of the unstable modes can balance, and the $\Lambda(\epsilon)$ curve is smooth across the melting (in fact LJ₁₇ shows no signature of melting according to this measure [42]). This conjecture can be tested by studies of the larger clusters with calculations of the participation ratios of the unstable modes, which will clarify their role in the chaoticity of a dynamical system.

One may intuitively expect that unstable modes (i.e., negative curvatures) cause the dynamics to be chaotic. As noted by Dellago and Posch in their study of melting in two-dimensional systems [22], the fraction of unstable modes, which is a rough measure of negative curvatures, has a similar dependence on the parameters as Λ . These unstable modes can, however, become important only when particles are capable of large-scale motion. (In a related context, it has been seen [30] that Λ falls when a liquid is cooled through its glass-transition temperature, namely, as the unstable modes becomes localized [41].)

Using the framework of a geometric theory of Hamiltonian chaos, we computed an estimate for the Lyapunov exponent from the curvature of the potential-energy surface and its fluctuation. We studied the variation of these quantities with the temperature of the system, and found that the mean curvature is always a monotonic function of energy but the variance has a simple energy dependence only for smaller clusters. In the coexistence region of 13 particle clusters—these are the cases in which the potential-energy surface has a deep global minimum which is well separated from the next lowest structure— σ is nonmonotonic. The LJ bulk system shows a singular behavior for σ at melting, which may indicate some sort of topological change in the configuration space [13].

The resulting estimate λ is generally larger than Λ in the solid phase. For bulk, the discrepancy is small, but for clus-

ters, the agreement is only qualitative. Curvature fluctuations for clusters are correlated, and this effectively reduces the parametric instability in the dynamics. The spectral features of the curvature fluctuations such as bandwidth are not well accounted for by the geometric theory even for the bulk system. At higher temperatures λ is lower than Λ , which is attributed to the unstable modes (negative curvatures) which are ignored in the geometric theory. The contribution of the unstable modes toward chaoticity (obtained by subtracting λ from Λ and therefore only approximate) is small in the solid phase, but can be as large as one-third in the liquid phase. Since σ and k do not show any singularity at melting for clusters, the parametric contribution coming from the change in topography of the potential-energy surface changes smoothly. Therefore, the fractional chaoticity coming from the unstable modes, $\delta\lambda_u$, also seems to vary continuously with energy.

In summary, our application of the geometric theory to the dynamics of the melting transition for cluster and bulk systems has provided a satisfactory qualitative understanding of the underlying mechanisms in terms of the change in roughness of the potential-energy surface, curvature fluctuations, and parametric instability. While agreement between theory and simulation is reasonable for the bulk system, for the case of finite clusters the situation is less satisfactory. The main source of the discrepancy seems to lie in the fact that, in cluster systems, correlations are temporally long lived. This aspect must be incorporated within the present framework of the geometric theory (see, e.g., Refs. [33,36]) in order to achieve quantitative accuracy.

ACKNOWLEDGMENTS

We thank Srikanth Sastry for discussions, generous advice, and for a critical reading of the manuscript. This work was supported by Grant No. SPS/MO-5/92 from the Department of Science and Technology.

-
- [1] See, e.g., R. S. Berry, *Chem. Rev.* **93**, 2379 (1993); D. J. Evans, E. G. D. Cohen, and G. P. Morriss, *Phys. Rev. A* **42**, 5990 (1990); C. Seko and K. Takatsuka, *J. Chem. Phys.* **104**, 8613 (1996).
- [2] R. P. Gupta, *Phys. Rev. B* **23**, 6265 (1981).
- [3] L. Casetti, C. Clementi, and M. Pettini, *Phys. Rev. E* **54**, 5969 (1996); see also L. Casetti, R. Livi, and M. Pettini, *Phys. Rev. Lett.* **74**, 375 (1995).
- [4] S. Sastry, *Phys. Rev. Lett.* **76**, 3738 (1996).
- [5] C. Chakravarty and R. Ramaswamy, *J. Chem. Phys.* **106**, 5564 (1997).
- [6] A. J. Lichtenberg and M. A. Lieberman, *Regular and Chaotic Dynamics*, 2nd ed. (Springer-Verlag, Berlin, 1992).
- [7] M. Pettini and M. Landolfi, *Phys. Rev. A* **41**, 768 (1990).
- [8] E. Fermi, J. Pasta, and S. Ulam (unpublished); and in *Collected Papers of Enrico Fermi*, edited by E. Segre (University of Chicago Press, Chicago, 1965), Vol. 2.
- [9] H. A. Posch and W. G. Hoover, *Phys. Rev. A* **39**, 2175 (1989).
- [10] R. J. Hinde and R. S. Berry, *J. Chem. Phys.* **99**, 2942 (1993); R. J. Hinde, R. S. Berry, and D. J. Wales, *ibid.* **96**, 1376 (1992).
- [11] S. Sastry (private communication).
- [12] P. Butera and G. Caravati, *Phys. Rev. A* **36**, 962 (1987).
- [13] L. Caiani, L. Casetti, C. Clementi, and M. Pettini (unpublished).
- [14] S. Flach and G. Mutschke, *Phys. Rev. E* **49**, 5018 (1994).
- [15] G. Benettin and A. Tenenbaum, *Phys. Rev. A* **28**, 3020 (1983); A. Tenenbaum and R. Simonazzi, *Phys. Rev. E* **54**, 964 (1996).
- [16] V. Mehra and R. Ramaswamy (unpublished).
- [17] C. Alabiso, N. Besagni, M. Casartelli, and P. Marenzoni, *J. Phys. A* **29**, 3733 (1996).
- [18] S. K. Nayak, R. Ramaswamy, and C. Chakravarty, *Phys. Rev. E* **51**, 3951 (1995).
- [19] J. P. Labastie and R. L. Whetten, *Phys. Rev. Lett.* **65**, 1567 (1990).
- [20] V. Mehra, S. K. Nayak, and R. Ramaswamy, *Pramana J. Phys.* **48**, 603 (1997).

- [21] V. Mehra and R. Ramaswamy (unpublished).
- [22] Ch. Dellago and H. A. Posch, *Physica A* **230**, 364 (1996).
- [23] A. Bonasera, V. Latora, and A. Rapisarda, *Phys. Rev. Lett.* **75**, 3434 (1995).
- [24] S. K. Nayak, A. Bhattacharya, P. Jena, and S. D. Mahanti (unpublished).
- [25] S. Sawada and S. Sugano, *Z. Phys. D* **14**, 247 (1989).
- [26] S. K. Nayak, R. Ramaswamy, and C. Chakravarty, *Phys. Rev. Lett.* **74**, 4181 (1995).
- [27] A. Bulgac (unpublished).
- [28] C. Amitrano and R. S. Berry, *Phys. Rev. E* **47**, 3158 (1993).
- [29] U. Salian, S. N. Behera, and V. Ramamurthy, *J. Chem. Phys.* **105**, 3679 (1996).
- [30] S. K. Nayak, P. Jena, K. Ball, and R. S. Berry (unpublished).
- [31] M. Gutzwiller, *Classical and Quantum Chaos* (Springer-Verlag, Berlin, 1990).
- [32] M. Pettini, *Phys. Rev. E* **47**, 828 (1993).
- [33] S. Chaudhuri, G. Gangopadhyay, and D. S. Ray, *Phys. Rev. E* **47**, 311 (1993).
- [34] D. M. Barnett, T. Tajima, K. Nishihara, Y. Ueshima, and H. Furukawa, *Phys. Rev. Lett.* **76**, 1812 (1996).
- [35] M. Toda, *Phys. Lett. A* **48**, 335 (1974); P. Brumer and J. W. Duff, *J. Chem. Phys.* **65**, 3566 (1976).
- [36] N. G. Van Kampen, *Phys. Rep.* **24**, 71 (1976).
- [37] L. Casetti and A. Macchi, *Phys. Rev. E* **55**, 2539 (1997).
- [38] R. LaViolette and F. H. Stillinger, *J. Chem. Phys.* **83**, 4079 (1985).
- [39] J. E. Adams and R. M. Stratt, *J. Chem. Phys.* **93**, 1332 (1990).
- [40] T. L. Beck and T. L. Marchiro, *J. Chem. Phys.* **93**, 1347 (1990).
- [41] S. D. Bembenck and B. B. Laird, *Phys. Rev. Lett.* **74**, 936 (1995).
- [42] G. M. Tanner, A. Bhattacharya, S. K. Nayak, and S. D. Mahanti, *Phys. Rev. E* **55**, 322 (1997).